Inorganic Chemistry

Article

pubs.acs.org/IC

Metal Ion Binding by a G-2 Poly(ethylene imine) Dendrimer. Ion-Directed Self-Assembling of Hierarchical Mono- and Two-Dimensional Nanostructured Materials

Carla Bazzicalupi,[†] Antonio Bianchi,*[,†] Claudia Giorgi,[†] Paola Gratteri,[‡] Palma Mariani,[†] and Barbara Valtancoli[†]

[†]Department of Chemistry "Ugo Schiff", University of Florence, Via della Lastruccia 3, 50019 Sesto Fiorentino, Italy

[‡]Department of NEUROFARBA, Pharmaceutical and Nutraceutical Section, and Laboratory of Molecular Modeling Cheminformatics & QSAR, University of Florence, Via Ugo Schiff 6, 50019 Sesto Fiorentino, Italy

Supporting Information

ABSTRACT: The second-generation poly(ethylene imine) dendrimer (L), based on ammonia as the initiating core molecule, forms stable metal complexes in aqueous solution. Speciation of the complex species formed and determination of the relevant stability constants were performed by means of potentiometric titration in 0.10 M NMe_4Cl solution at 298.1 K. The interaction of L with Ni^{2+}, Cu^{2+}, Zn^{2+}, Cd^{2+}, and Pb^{2+} gives rise to stable complexes with 1:1 (all metal ions), 2:1 (Ni^{2+}, Cu^{2+}, Zn^{2+}, Cd^{2+}), 3:2 (Ni^{2+}, Zn^{2+}, Cd^{2+}), and 3:1 (Cu^{2+}) metal/ligand stoichiometries. The crystal structures of $[Ni_3L_2](ClO_4)_6 \cdot 6H_2O$ (**1**) and $[Cu_3LCl(OH)_{0.5}(NO_3)_{0.5}ox]$-$Cl_{1.5}(NO_3)_{0.5} \cdot 5.5H_2O$ (**2**) were solved by X-ray diffraction. The $Ni_3L_2^{6+}$ complex cation in **1**, existing in solution as a very stable species, shows two dendrimer units linked together by a bridging Ni^{2+} ion. In **2**, the Cu_3L^{6+} complex cation, which also exists in solution as a very stable species, gives rise, via bridging coordination of oxalate anions, to nanostructured polymeric chains that self-organize into two-dimensional sheets. In both structures, the hierarchical mono- and two-dimensional aggregation is triggered by the action of ionic species behaving either as functional groups on the dendrimer surface (metal ions) or as the glue (metal ions, oxalate) that sticks together dendrimer units. Two association routes, developing via coordinative forces, guide the directional aggregation of dendrimer units: (a) aggregation via metal ions shared by the surfaces of contiguous dendrimer molecules and (b) aggregation via chelating ligands bridging surface metal ions pertaining to contiguous dendrimer molecules. Such aggregation modes provide coordinative routes for the self-assembly of novel families of nanostructured functional materials.

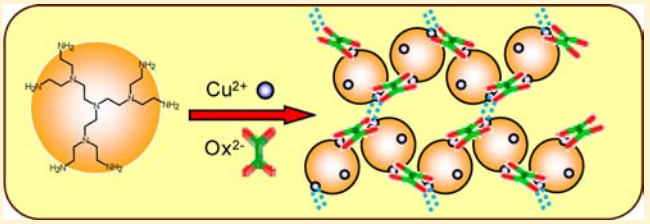

INTRODUCTION

Dendrimers are three-dimensional compounds formed by reiterated reaction sequences starting from smaller "core" molecules and proceeding via discrete "Aufbau" stages,[1] referred to as generations (G) (Figure 1). Dendrimer chemistry is well-established[2,3] and continues to develop at a pace due to the surge of applications that dendrimers have already found, or promise to implement, in important scientific and technological areas, including gene[4] and drug delivery,[5] medicinal chemistry,[6] sensing,[7] and advanced materials.[8]

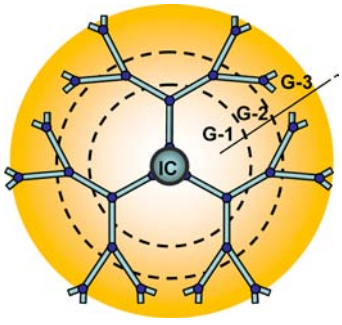

Figure 1. Growth of dendrimer generations (G-1, G-2,...) from an initiating core (IC).

In contrast to other types of macromolecules, dendrimers are generally characterized by highly ordered, well-defined structures produced by the iterative synthetic procedures adopted to grow the dendritic architecture around the central core. Lower-generation dendrimers can be thought of as flexible molecules with no appreciable inner regions, whereas medium-sized (G-3 or G-4) have an internal space that is essentially separated from the outer shell of the dendrimer. Very large (G-7 and greater) dendrimers can be thought of more like solid particles with very dense surfaces due to the crowding of branches in the outer shell. The iterative synthetic strategies allow the introduction in a highly repetitive and uniform

Received: November 19, 2012
Published: February 6, 2013

   dx.doi.org/10.1021/ic3025292 | *Inorg. Chem.* 2013, 52, 2125−2137

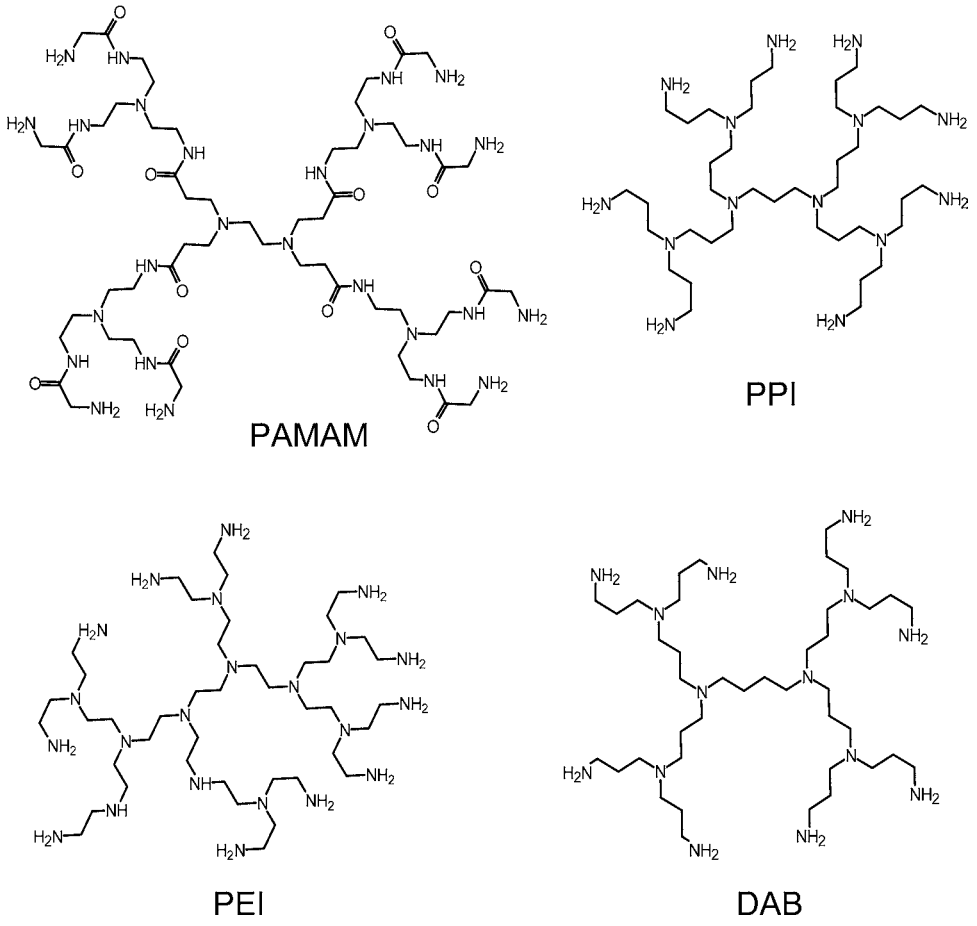

Figure 2. Poly(amido amine) (PAMAM), poly(propylene imine) (PPI), poly(ethylene imine) (PEI), and poly(propylene imine) diaminobutane (DAB) dendrimers.

manner of functional groups onto the dendrimer surface and into the dendrimer structure. Such an accumulation of identical functional groups within the dendrimer molecule gives rise to amplification of these functionalities, a property that largely contributes to defining the peculiarity of this class of compounds. If, on the one hand, the concentration of active sites is a favorable outcome of dentritic structures, allowing, for instance, the preparation of materials with high catalyst-to-dendrimer ratios,[2c] on the other hand, it may complicate the analysis of dendrimer properties at the molecular level. Similar difficulties can be encountered, for instance, when the binding properties of dendrimers containing amino groups are being studied. Examples of dendrimers bearing amino functionalities, such as the poly(amido amine) (PAMAM), the poly(propylene imine) (PPI), the poly(ethylene imine) (PEI), and the poly(propylene imine) diaminobutane (DAB) compounds, some of which are commercially available, are shown in Figure 2.

These dendrimers have been shown to form complexes with metal ions.[9−29] Their binding ability has usually been studied by approaching the ligand coordinative saturation, that is, by leading the ligand to bind as many metal ions as possible. In this way, dendrimers have shown the best of their metal coordination potentiality, revealing them to be able to bind enormous numbers of metal ions per ligand molecules, on the scale of their molecular size.[13−15,19,21−23] Despite the large number of metal ions in such dendrimer complexes, information about metal coordination environments and pH dependence of complexation reactions has been obtained since the earliest studies.[9,11] Moreover, attempts to perform the speciation of the complex systems and determining the equilibrium constants for complexation equilibria with PEI dendrimers and metal ions, such as Cu^{2+}, Ni^{2+}, Mn^{2+}, Cd^{2+}, Pb^{2+}, and Hg^{2+}, were made by considering the repeating triamine units of the dendrimer as identical independent ligand molecules, under the implicit assumption that these repeating units were uniformly distributed in solution, in contrast to their actual localization within the same dendrimer molecule.[19,28] Also, these studies were performed under conditions approaching the ligand coordinative saturation, the metal-to-triamine unit ratios being close to 1:1 and extending, at most, up to 1:4. Despite the approximation of considering the repeating units of a dendrimer as independent ligand molecules, the results of these studies were functional to the purposes for which they were developed, as, for instance, the application of PEI dendrimers to sequestration and recovery of solution metal ions.[28]

Nevertheless, the study of metal ion complexation properties of dendrimers under, or close to, coordinative saturation of the ligand leads to incomplete information. First of all, it leads to the identification a limited number of complex species relative to the many that a dendrimer should be able to form. For instance, a dendrimer containing a large number of amino groups, like those shown in Figure 2, is expected to form metal complexes in which the ligand in a high protonation state binds

dx.doi.org/10.1021/ic3025292 | Inorg. Chem. 2013, 52, 2125−2137

few metal ions. Some of the missing species might hold pleasant surprises in terms of chemical properties.

Dendrimers also represent a good opportunity to generate hierarchical structures that are self-assembled through the action of different supramolecular forces.[29,30] It was recently shown,[29] for instance, that the assembly of nanofibers based on a G-4 amino-terminated PPI dendrimer can be achieved in water by using determined ions in an active way, Cd^{2+} and acetate (AcO^-) in the specific case. Cd^{2+} ions coordinate to the surface primary amine groups of the dendrimer, but they are not able to complete their coordination spheres by using dendrimer donor atoms. In such conditions, these metal ions adorning the dendrimer surface may attract chelating acetate ions that approach (bind) the metal ions through their carboxylate heads and project their aliphatic ($-CH_3$) tails into the surrounding aqueous medium. Such cascade-like coordination produces a hydrophobic modification of the dendrimer surface, which was shown to be responsible for the association of the dendrimer complex units into fibers. As shown by molecular dynamic simulations, the AcO^- anions act as an "ionic glue" that solidifies (clusters) at the interface between contiguous units, stabilizing the fiber.[29]

In the present work, we describe the metal ion binding properties of the low-molecular-weight dendrimer L, a G-2 PEI molecule that was first synthesized by Tomalia.[31] The results obtained by performing a detailed analysis of binding equilibria showed that L is actually a good receptor for metal ions, such as Ni^{2+}, Cu^{2+}, Zn^{2+}, Cd^{2+}, and Pb^{2+}. In particular, it gives rise to the formation of metal complexes with a variety of stoichiometries, including species with 1:1, 2:1, 3:1, and 3:2 metal/ligand molar ratios. Furthermore, L is able to self-assemble hierarchically ordered aggregations, as shown by the crystal structures of $[Ni_3L_2](ClO_4)_6{\cdot}6H_2O$ and $[Cu_3LCl(OH)_{0.5}(NO_3)_{0.5}ox]Cl_{1.5}(NO_3)_{0.5}{\cdot}5.5H_2O$, in which dendrimeric complex units are linked together, thanks to the active participation of ionic species, to form mono- and two-dimensional aggregates.

As shown here, the talent of this small dendrimer does not betray the reputation of its higher-generation congeners and suggests binding equilibria and self-association schemes that should be also effective, and possibly amplified, for higher-generation dendrimers.

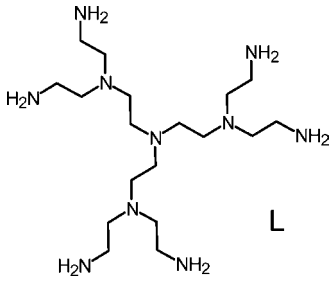

EXPERIMENTAL SECTION

General Information. Unless otherwise specified, all starting materials were purchased from commercial sources and used as supplied. Tosyl aziridine used in the synthesis of L was prepared as previously described.[32] Pale blue crystals of $[Ni_3L_2](ClO_4)_6{\cdot}6H_2O$ suitable for X-ray diffraction analysis were obtained by slow evaporation at room temperature of an aqueous solution containing $Ni(ClO_4)_2{\cdot}6H_2O$ and L in a 3:2 molar ratio at pH 11. ***Caution!*** *Perchlorate salts of metal complexes with organic ligands are potentially explosive. Only a small amount of material should be prepared and must be handled with care.* Deep blue crystals of $[LCu_3Cl(OH)_{0.5}(NO_3)_{0.5}ox]Cl_{1.5}(NO_3)_{0.5}{\cdot}5.5H_2O$ (ox = oxalate) suitable for X-ray diffraction analysis were obtained by slow evaporation at room temperature of an aqueous solution prepared from $Cu(NO_3)_2{\cdot}3H_2O$, L, and oxalic acid in a 3:2:3 molar ratio at pH 8.

Synthesis of the Ligand. The ligand L was synthesized, according to a slight modification of a reported procedure.[31] A solution of tosyl aziridine (0.6 mol) in absolute ethanol (300 cm^3) was added dropwise to a vigorously stirred solution of tris(2-aminoethyl)amine (0.1 mol) in 50 cm^3 of absolute ethanol over 3 h at room temperature. Stirring was maintained for an additional 5 h, after which the white suspension was filtered, and the solid residue, consisting of the hexatosylated derivatives of the ligand, was thoroughly washed with ethanol and dried in vacuum at 40 °C. Yield: 88%. The tosyl groups were removed by using concentrated sulfuric acid. The tosylated compound (10 g) was dissolved in warm concentrated sulfuric acid (100 cm^3), and the solution was kept at 115 °C for 70 h. The solution was then cooled to room temperature and cautiously added to 500 cm^3 of ice-cold diethylether under stirring. The solid compound separated from the solution was filtered, washed several times with cold diethylether, and dried in vacuum at room temperature. The compound was successively dissolved in the minimum amount of water and eluted though a column filled with a Dowex 1 × 8 (20−50 mesh) exchange resin in the alkaline form to obtain the free ligand, as an oily amine, after removing water from the recovered solution by vacuum evaporation. The compound was isolated as $L{\cdot}10HCl{\cdot}1.5H_2O$ by treating the oily amine in ethanol with concentrated HCl. Yield: 85%. ^1H NMR (D_2O, pH 2.8, 400 MHz): δ 3.49 (6H, t), 3.19 (12H, t), 3.12 (6H, t), 2.94 (12H, t). Elemental analysis of $L{\cdot}10HCl{\cdot}1.5H_2O$ (%): Calcd for $C_{18}H_{61}N_{10}O_{1.5}Cl_{10}$: C, 27.15; N, 17.59; H, 7.72. Found: C, 27.11; N, 17.59; H, 7.80. ESI-MS: m/z = 405.4 ($[M + H]^+$), 362.4 ($[M - (-CH_2CH_2NH_2)]^+$).

Potentiometric Measurements. Potentiometric (pH-metric) titrations, performed to determine equilibrium constants, were performed by using an automated system composed of a 50 cm^3 reaction vessel, water-thermostatted at 298.1 ± 0.1 K, mounted on a Metrohm 728 stirrer, and equipped with a combined Metrohm 6.0262.100 electrode and a source of nitrogen presaturated with 0.1 M NMe_4Cl to maintain an inert atmosphere into the vessel during the measurements. The titrant was delivered by a Metrohm 765 Dosimat buret, while the potentiometric measurements were made with a Metrohm 713 pH meter. The acquisition of the emf data was performed with the computer program PASAT.[33] The electrode was calibrated as an hydrogen-ion concentration probe by titration of previously standardized amounts of HCl with CO_2-free NaOH solutions and determining the equivalent point by Gran's method,[34] which gives the standard potential, $E°$, and the ionic product of water (pK_w = 13.83(1) in 0.1 M NMe_4Cl at 298.1 K). The computer program HYPERQUAD[35] was used to calculate ligand protonation and complex stability constants. The pH range investigated was 2.5−11.0. The concentration of the ligand was 1 × 10^{-3} M in all measurements. The concentration of metal ions was varied in the ranges of $0.5[L] \le [Ni^{2+}] \le 2.5[L]$, $0.5[L] \le [Cu^{2+}] \le 3.5[L]$, $0.5[L] \le [Zn^{2+}] \le 2.5[L]$, $0.5[L] \le [Cd^{2+}] \le 2.5[L]$, and $0.5[L] \le [Pb^{2+}] \le 1.5[L]$ for the determination of metal complex stability constants. Precipitation of metal hydroxides was observed for $[Ni^{2+}] > 1.6[L]$, $[Cu^{2+}] > 3[L]$, $[Zn^{2+}] > 1.8[L]$, and $[Cd^{2+}] > 1.6[L]$. In the case of Pb^{2+}, precipitation of hydroxide was observed above pH 10 in all measurements. The portions of the relevant titrations prior to precipitation were included into the calculations. In the case of Ni^{2+}, some slowness was observed in achieving the equilibrium during titrations above pH 4. Preliminary measurements showed that a waiting time of 30 min after each titrant addition was enough to ensure the achievement of the equilibrium before starting with the normal procedure for the acquisition of potentiometric readings. Accordingly, such a waiting time was adopted for all titrations involving Ni^{2+} complexation above pH 4. Because of the great stability of the $Ni_3L_2^{6+}$ complex competing with the formation of Ni_2L^{4+} and Ni_2LOH^{3+}, the determination of the equilibrium constants for the formation of such binuclear species was only possible by performing titrations with metal-to-ligand molar ratios close to 1.6, but not greater than this value

dx.doi.org/10.1021/ic3025292 | Inorg. Chem. 2013, 52, 2125−2137

to avoid precipitation of metal hydroxide (see above). Three titrations in the case of Pb^{2+}, four in the case of Zn^{2+} and Cd^{2+}, and five in the case of Ni^{2+} and Cu^{2+} were used to determine metal complexation constants. For all complex systems, the different titration curves were treated as separated curves without significant variations in the values of the common stability constants. Finally, the sets of data were merged together and treated simultaneously to give the final stability constants. The hydrolysis of metal ions was considered in the calculations. Different equilibrium models for the complex systems were generated by eliminating and introducing different species. Only those models for which the HYPERQUAD program furnished a variance of the residuals $\sigma^2 \leq 9$ were considered acceptable. Such a condition was unambiguously met by a single model for each system.

Calorimetric Measurements. Ligand protonation enthalpies were determined in 0.10 M NMe_4Cl solution by means of isothermal titration calorimetry using a TAM III (TA Instrument) microcalorimeter equipped with a precision Lund syringe pump coupled with a 0.250 cm^3 gastight Hamilton syringe. The microcalorimeter was checked by determining the enthalpy of reaction of strong base (NMe_4OH) with strong acid (HCl) solutions. The value obtained (−56.7(2) kJ/mol) was in agreement with the literature values.[36] Further checks were performed by determining the enthalpies of protonation of ethylenediamine. In a typical experiment, a NMe_4OH solution (0.10 M, addition volumes 10 μL) was added to acidic solutions of the ligands (5×10^{-3} M, 1.2 cm^3). Corrections for heats of dilution were applied. The corresponding enthalpies of reaction were determined from calorimetric data by means of the HypΔH program.[37]

Spectroscopic Measurements. UV−vis spectra were recorded at 298 K on a Jasco V-670 spectrophotometer. The solutions of Ni^{2+} and Cu^{2+} complexes were prepared from appropriate amounts of metal chloride standard solutions and L·10HCl·1.5H_2O. The solutions used for recording the spectra of mononuclear complexes were prepared in the presence of a 2-fold excess of ligand ([L] = 2[M^{2+}]) to depress the formation of complexes with a metal-to-ligand stoichiometry different from 1:1. In the cases of spectra recorded at different pHs with the same sample, the initial solution was alkaline and the pH was lowered by small additions of gaseous HCl, without changing the sample volume. Equilibration of samples containing Ni^{2+} complexes, for which slow complexation reactions were observed, was performed by keeping the sealed samples at 50 °C during 15 min, followed by a minimum of 30 min at room temperature. ^1H NMR spectra (400 MHz) in D_2O solution were recorded at 298 K on a 400 MHz Bruker Avance III spectrometer. In experiments carried out at different pH values, small amounts of 0.01 M NaOD and DCl were added to the solution to adjust the pD. The solution pH can be calculated from the measured pD value by means of the formula: pH = pD − 0.40.[38]

Crystallography. Mauve $[Ni_3L_2](ClO_4)_6·6H_2O$ (a) and blue $[Cu_3LCl(OH)_{0.5}(NO_3)_{0.5}ox]Cl_{1.5}(NO_3)_{0.5}·5.5H_2O$ (b) single crystals were used for X-ray diffraction analysis. A summary of the crystallographic data is reported in Table S1 (Supporting Information), while ORTEP drawings of the structures displaying the thermal ellipsoids are shown in Figure S1 of the Supporting Information. The integrated intensities were corrected for Lorentz and polarization effects, and empirical absorption correction was applied by means of the ABSPACK program.[39] The structures were solved by direct methods (SIR2004).[40] Refinements were performed by means of full-matrix least-squares using the SHELX-97 program.[41] All the non-hydrogen atoms were anisotropically refined while the hydrogen atoms linked to the carbon atoms and nitrogen atoms were introduced in calculated positions, and their coordinates were refined according to the linked atoms. (a) Two of the three perchlorate anions belonging to the asymmetric unit are affected by rotational disorder (Cl1 and Cl3), and some of their oxygen atoms were found in double positions and introduced with partial population parameter. (b) The crystal is a 1:1 solid solution of $[Cu_3LCl(OH)ox]Cl_{1.5}(NO_3)_{0.5}·5.5H_2O$ and $[Cu_3LCl(NO_3)ox]Cl_{1.5}(NO_3)_{0.5}·5.5H_2O$. A chloride and a nitrate, which were found to share almost the same position, as well as a water molecule close to the coordinated nitrate, were refined with a 0.5 population parameter.

Molecular Modeling. Investigation of the solvated ZnH_5L^{7+} complex was carried out by means of the empirical force field method (AMBER3),[42] followed by QM/MM calculations performed by using the Qsite software.[43] The QM region comprised the protonated ligand, the metal center, and the coordinated water molecule and was treated at the DFT/B3LYP[44] level of theory with the LACVP* basis set,[45] whereas the MM region comprised the water solvent molecules and was treated with Impact,[46] OPLS2005 force-field.

RESULTS AND DISCUSSION

Ligand Protonation Behavior. Polyamine ligands can bind metal ions when they contain a sufficient number of not-protonated nitrogen atoms. Accordingly, the determination of ligand protonation constants is preliminary to metal ion coordination studies.

L contains six primary and four tertiary amine groups that can be involved in protonation equilibria. In the pH range (2.5−11) investigated in this work, however, only eight out of these amine groups undergo protonation. This is a common behavior of polyamines containing many protonation sites at a close distance from each other, since the accumulation of positive charge occurring upon successive protonation may cause the last protonation stages to occur in very acidic solution, out of the pH range useful for the determination of the relevant protonation constants by the potentiometric method.[47] The corresponding protonation constants, obtained in 0.10 M NMe_4Cl aqueous solution at 298.1 K, are listed in Table 1 along with the corresponding enthalpy changes,

Table 1. Protonation Constants of L in 0.10 M Me_4NCl at 298.1 ± 0.1 K

	log K	$\Delta H°$ (kJ/mol)	$T\Delta S°$ (kJ/mol)
$L + H^+ = HL^+$	10.16(2)[a]	−52.4(3)	5.6(3)
$HL^+ + H^+ = H_2L^{2+}$	9.98(1)	−46.2(3)	10.7(3)
$H_2L^{2+} + H^+ = H_3L^{3+}$	9.25(3)	−50.9(5)	1.9(5)
$H_3L^{3+} + H^+ = H_4L^{4+}$	9.22(2)	−52.8(3)	−0.2(3)
$H_4L^{4+} + H^+ = H_5L^{5+}$	8.57(2)	−52.7(2)	−3.8(2)
$H_5L^{5+} + H^+ = H_6L^{6+}$	8.32(1)	−53.6(2)	−6.1(2)
$H_6L^{6+} + H^+ = H_7L^{7+}$	5.69(2)	−37.5(2)	−5.0(2)
$H_7L^{7+} + H^+ = H_8L^{8+}$	2.60(2)	−23.5(4)	−8.7(4)

[a]Values in parentheses are the standard deviations on the last significant figures.

determined by isothermal titration calorimetry, and the relevant entropic terms. As can be seen from this table, the first six constants are very high, ranging from log K = 10.16 to log K = 8.32, and accompanied by highly favorable enthalpic contributions ($-\Delta H°$ in the range of 46.2−53.6 kJ/mol). A gap of 2.63 logarithmic units separates this group of protonation constants from the seventh protonation constant, which is greater by 3.09 logarithmic units than the eighth one, the last two protonation stages being characterized by a lower exothermicity ($-\Delta H°$ = 37.5 and 23.5 kJ/mol, respectively). The values of these protonation constants and their distribution, as well as the relevant enthalpy changes, are consistent with the first six protonation stages taking places on the primary amine groups, the successive two stages involving tertiary nitrogens.[47] ^1H NMR spectra recorded at different pH values (Figure S2 in Supporting Information) confirmed this protonation pattern. In particular, they showed that the seventh protonation stage involves the central tertiary nitrogen of the ligand while, upon binding of the eighth proton, a redistribution of positive charge (protonation) from this nitrogen to the three

dx.doi.org/10.1021/ic3025292 | Inorg. Chem. 2013, 52, 2125−2137

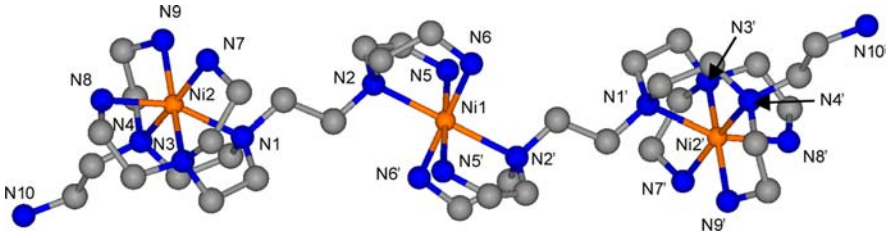

Figure 3. Crystal structure of the complex $Ni_3L_2^{6+}$.

Table 2. Selected Distances and Angles in the Crystal Structure of $[Ni_3L_2](ClO_4)_6 \cdot 6H_2O$

distances (Å)		angles (deg)			
Ni1−N5	2.13(1)	N5−Ni1−N2	83.0(4)	N3−Ni2−N1	83.6(3)
Ni1−N2	2.185(9)	N5−Ni1−N6	91.2(3)	N3−Ni2−N8	81.7(3)
Ni1−N6	2.144(9)	N5−Ni1−N2′	97.0(4)	N3−Ni2−N4	108.3(3)
Ni1−N2′	2.185(9)	N5−Ni1−N6′	88.8(3)	N3−Ni2−N9	169.8(4)
Ni1−N6′	2.144(9)	N5−Ni1−N5′	180.0(4)	N3−Ni2−N7	80.8(3)
Ni1−N5′	2.13(1)	N2−Ni1−N6	81.9(3)	N1−Ni2−N8	160.4(3)
Ni2−N3	2.128(9)	N2−Ni1−N2′	180.0(3)	N1−Ni2−N4	80.8(3)
Ni2−N1	2.209(9)	N2−Ni1−N6′	98.1(3)	N1−Ni2−N9	102.6(4)
Ni2−N8	2.109(8)	N2−Ni1−N5′	97.0(4)	N1−Ni2−N7	97.7(3)
Ni2−N4	2.286(8)	N6−Ni1−N2′	98.1(3)	N8−Ni2−N4	91.5(3)
Ni2−N9	2.107(9)	N6−Ni1−N6′	180.0(3)	N8−Ni2−N9	93.9(4)
Ni2−N7	2.162(8)	N6−Ni1−N5′	88.8(3)	N8−Ni2−N7	92.7(3)
		N2′−Ni1-N6′	81.9(3)	N4−Ni2−N9	80.8(3)
		N2′−Ni1-N5′	83.0(4)	N4−Ni2−N7	170.4(3)
		N6′−Ni1-N5′	91.2(3)	N9−Ni2−N7	90.3(3)

surrounding tertiary nitrogens occurs, in agreement with previous results[48] obtained by means of ^{15}N NMR measurements for protonation of PPI dendrimers. This means that, in H_8L^{8+}, the central tertiary nitrogen is less involved in protonation than in H_7L^{7+}.

Also, the variation of entropic contributions to protonation processes, shifting from favorable to unfavorable with increasing protonation, is typical of polyamines. Upon successive protonation, the favorable entropy contribution due to proton desolvation is overcome by two entropy consuming phenomena determined by the accumulation of positive charge on the molecule: the increasing stiffening of its structure and the increasing attraction exerted on the polar solvent molecules.[47]

Crystal Structure of $[Ni_3L_2](ClO_4)_6 \cdot 6H_2O$. The crystal structure consists of a trinuclear $[Ni_3L_2]^{6+}$ complex cation (Figure 3), perchlorate anions, and water solvent molecules. Bond distances and angles for metal coordination environments are included in Table 2. The central nickel ion (Ni1) lies on a crystallographic inversion center and is coordinated to the nitrogen atoms of two triamine branches, each belonging to one of the symmetry-related ligand molecules. The resulting octahedral coordination sphere of this metal ion is rather regular, the nitrogen atoms N2, N2′, N5, N5′ and N2, N2′, N6, N6′ defining, respectively, two planes that perfectly contain the nickel ion, and the coordination bond distances showing differences of, at most, 0.05(1) Å (Table 2). The remaining nitrogen atoms of each ligand molecule, but N10, form the coordination environment of the lateral symmetry-related metal ion (Ni2). The primary N10 nitrogen remains not coordinated and establishes H-bond contacts with solvent molecules and counterions. The coordination geometry of these metal ions can be described as a distorted octahedron, with the apical positions occupied by N4 and N7. The distance between the lateral symmetry related Ni^{2+} ions is 15.049(4) Å, and the overall length of the trinuclear $[Ni_3L_2]^{6+}$ complex is about 28.4 Å. This nanostructure, which also exists in aqueous solution as a very stable species (vide infra), is a lucid example of how dendrimers can be connected together to form more structured assemblies through the coordination of metal ions sharing the surfaces of contiguous molecules (Figure 4).

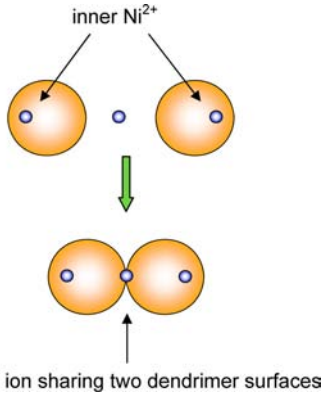

Figure 4. Schematic representation of the $Ni_3L_2^{6+}$ assembling: association of dendrimer molecules through coordination of a metal ion sharing surfaces.

Crystal Structure of $[Cu_3LCl(OH)_{0.5}(NO_3)_{0.5}ox]Cl_{1.5}(NO_3)_{0.5} \cdot 5.5H_2O$. The crystal structure is build up by $[Cu_3LCl(OH)_{0.5}(NO_3)_{0.5}ox]^{2+}$ (ox = oxalate) units, which give rise to a two-dimensional nanostructured polymer developing on the (202) plane, chloride and nitrate anions, and water solvent molecules. Figure 5a shows the $[Cu_3LCl(OH)_{0.5}(NO_3)_{0.5}ox]^{2+}$ unit, whereas selected bond angles and distances for the metal coordination environments are reported in Table 3. All ligand nitrogen atoms are involved in metal

dx.doi.org/10.1021/ic3025292 | Inorg. Chem. 2013, 52, 2125−2137

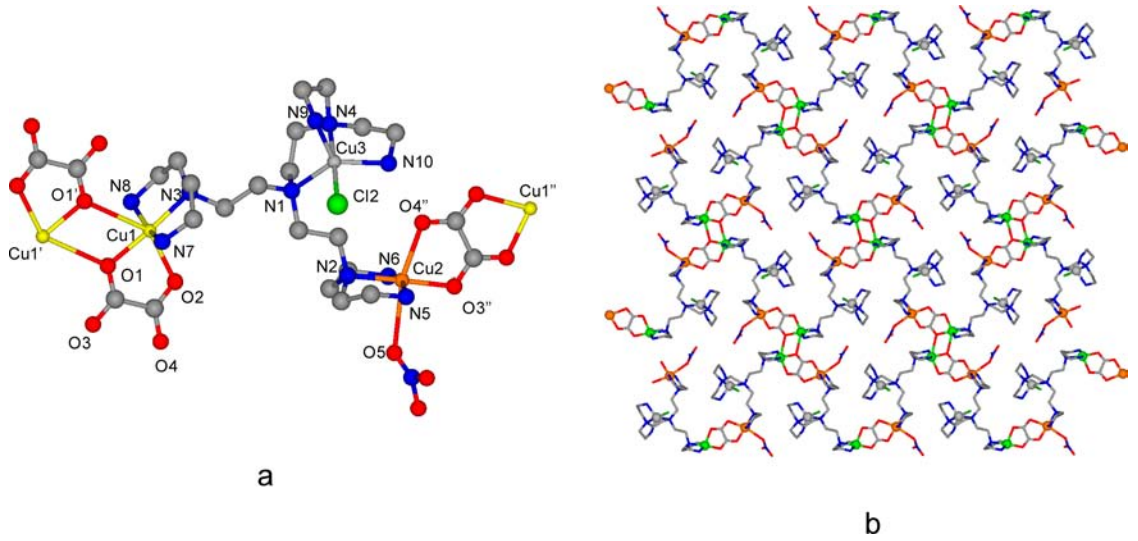

Figure 5. (a) Drawing of the $[Cu_3LCl(OH)_{0.5}(NO_3)_{0.5}ox]^{2+}$ unit (OH^- not shown), with metal center coordination geometries completed by symmetry-related linking groups (O1′,Cu1′ 1 − x, −y, −z; O3″,O4″, Cu1″ 0.5 − x, 0.5 + y, 0.5 − z). (b) 2D polymer growing on the (202) plane; Cu1 and Cu2 atoms represented as green and orange spheres, respectively.

Table 3. Selected Distances and Angles in the Crystal Structure of $Cu_3LCl(OH)_{0.5}(NO_3)_{0.5}ox]Cl_{1.5}(NO_3)_{0.5}\cdot 5.5H_2O$

distances (Å)							
Cu1−N3	2.041(3)	Cu2−N2	2.026(3)	Cu3−N1	2.227(3)	Cu1···Cu2	9.656(1)
Cu1−N7	1.996(3)	Cu2−N5	1.985(3)	Cu3−N4	2.028(3)	Cu1···Cu3	7.2708(7)
Cu1−N8	1.998(3)	Cu2−N6	1.990(3)	Cu3−N9	2.061(4)	Cu2···Cu3	5.5754(8)
Cu1−O1	2.009(2)	Cu2−O5	2.720(4)	Cu3−N10	2.074(3)	Cu1···Cu1′	4.1041(7)
Cu1−O2	2.257(3)	Cu2−O4′	2.273(2)	Cu3−Cl2	2.261(1)	Cu1″···Cu2	5.4793(6)
Cu1−O1′	2.849(3)	Cu2−O3′	2.004(3)				
angles (deg)							
N3−Cu1−N7	85.3(1)	N2−Cu2−N5	86.0(1)	N1−Cu3−N4	83.4(1)		
N3−Cu1−N8	85.4(1)	N2−Cu2−N6	86.4(1)	N1−Cu3−N9	115.3(1)		
N3−Cu1−O1	174.0(1)	N2−Cu2−O5	91.3(1)	N1−Cu3−N10	121.7(1)		
N3−Cu1−O2	106.8(1)	N2−Cu2−O4′	103.0(1)	N1−Cu3−Cl2	94.72(8)		
N3−Cu1−O1′	109.00(9)	N2−Cu2−O3′	177.9(1)	N4−Cu3−N9	84.3(1)		
N7−Cu1−N8	157.7(1)	N5−Cu2−N6	163.9(1)	N4−Cu3−N10	85.4(1)		
N7−Cu1−O1	91.2(1)	N5−Cu2−O5	83.6(1)	N4−Cu3−Cl2	177.8(1)		
N7−Cu1−O2	95.6(1)	N5−Cu2−O4′	95.6(1)	N9−Cu3−N10	120.1(1)		
N7−Cu1−O1′	84.5(1)	N5−Cu2−O3′	94.9(1)	N9−Cu3−Cl2	95.6(1)		
N8−Cu1−O1	96.1(1)	N6−Cu2−O5	82.3(1)	N10−Cu3−Cl2	96.53(9)		
N8−Cu1−O2	106.5(1)	N6−Cu2−O4′	100.0(1)				
N8−Cu1−O1′	79.4(1)	N6−Cu2−O3′	92.2(1)				
O1−Cu1−O2	78.31(9)	O5−Cu2−O4′	165.63(9)				
O1−Cu1−O1′	65.79(8)	O5−Cu2−O3′	87.0(1)				
O2−Cu1−O1′	144.09(9)	O4′−Cu2-O3′	78.79(9)				

binding. Each metal ion is coordinated to only one triamine branch of the ligand, the Cu3 cation also binding the innermost N1 atom. The coordination spheres of the three metal ions are completed by donors from exogenous species: three oxygen atoms from two different oxalate anions in the case of Cu1 and one chloride anion in the case of Cu3. In the case of Cu2, the coordination geometry is completed by two oxygen atoms of a chelating oxalate anion and by another oxygen atom belonging to either nitrate (shown in Figure 5) or hydroxide anions, which share the same position with partial population parameters. The overall coordination geometries of copper ions can be described as distorted octahedrons in the case of Cu1 (equatorial plane defined by the ligand donors N3, N7, N8 and the O1 oxalate oxygen) and Cu2 (equatorial plane defined by the ligand donors N2, N5, N6 and the O3″ oxygen from a symmetry related oxalate) and as a trigonal bipyramid in the case of Cu3 (apical positions defined by N4 and Cl2). All the $[Cu_3LCl(OH)_{0.5}(NO_3)_{0.5}ox]^{2+}$ units are joined by the oxalate group, which chelates Cu1 and Cu2 from different units (Cu2···Cu1″ 5.4793(6) Å), giving rise to monodimensional polymeric zigzag chains. In addition, the O1 oxygen atom of each oxalate group bridges symmetry-related Cu1 ions (Cu1···Cu1′ 4.1041(7) Å) and constitutes the connections between adjacent monodimensional polymeric chains to form two-dimensional sheets (Figure 5b) that are held together by hydrogen bonding involving intercalated water molecules and anions (counterions). As a consequence, each O1 atom occupies both, one of the equatorial positions of Cu1 (Cu1−

dx.doi.org/10.1021/ic3025292 | Inorg. Chem. 2013, 52, 2125−2137

O1 2.009(2)Å) and the apical position of Cu1′ (Cu1′-O1 2.849(3)Å), giving rise to a strongly asymmetric bridge. This is a relatively uncommon feature for the Cu-O-Cu group,[49] which, nevertheless, was observed in the tetranuclear $[Cu_4(ox)_8(H_2O)_2]^{8-}$ complex anion.[50]

It is to be noted that the Cu3 atom is not involved in the definition of the two-dimensional polymeric structure, which is instead determined by the tetranuclear secondary binding unit (SBU) constituted by two Cu1 and two Cu2 ions bridged by two oxalate anions (Figure 6a). The SBUs are then connected by dendrimer molecules (bearing Cu3), in such a way that a two-dimensional (4,4)-network is formed (Figure 6b).

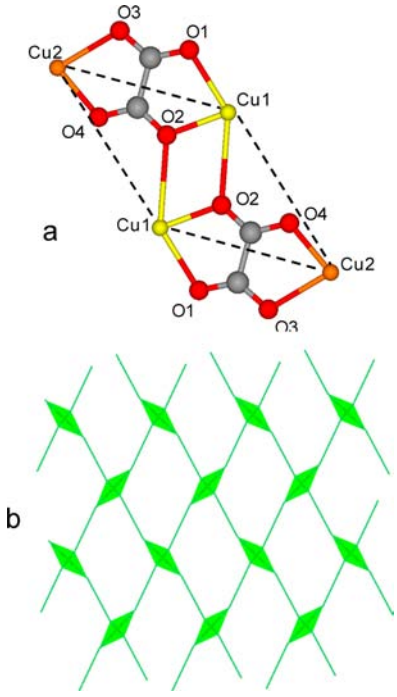

Figure 6. (a) Tetranuclear secondary binding unit (SBU). (b) 2D (4,4)-network.

Although the relatively small dimensions of the dendrimer make it difficult to define an inner region and a surface of the molecule, we can consider that the Cu1 and Cu2 ions, which bind to only one external triamine unit of the ligand and are available for the bridging coordination of oxalate, are localized at the surface of the dendrimer, while Cu3 occupies the inner region (Figure 7). Accordingly, the surface Cu^{2+} ions are the dendrimer functionalities responsible of the self-assembly of both mono- and two-dimensional hierarchically ordered structures, the oxalate ions acting as the glue that sticks together the components of the monodimensional ones and providing the additional cross-link anchorages for their self-organization into the two-dimensional ones (Figure 7).

Metal Ion Complexation. The three first-row transition-metal cations Ni^{2+}, Cu^{2+}, and Zn^{2+}; the second-row Cd^{2+}; and the post-transition Pb^{2+} were selected to disclose the coordination properties of L toward metal ions in aqueous solution. Speciation of these complex systems and determination of the relevant stability constants were performed by means of pH-metric (potentiometric) titrations (0.1 M Me_4NCl, 298.1 ± 0.1 K) and analysis of the associated data by means of the computer program HYPERQUAD,[35] which

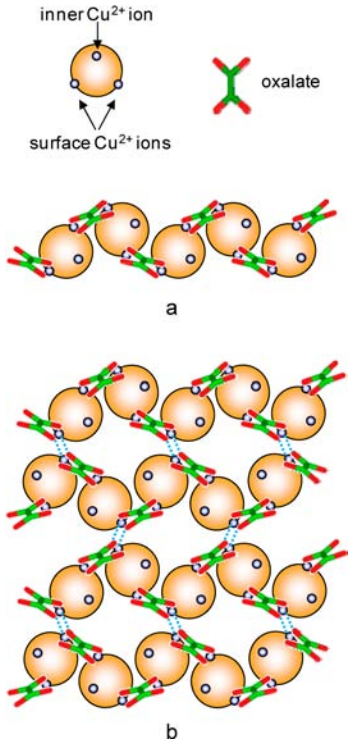

Figure 7. Oxalate anions direct both the self-assembly of monodimensional polymeric chains (a), through bridging coordination involving surface Cu^{2+} ions, and their self-organization to form two-dimensional polymeric sheets (b).

furnished the stability constants collected in Table 4. With the exclusion of Ni^{2+}, which required several minutes to reach the equilibrium (see the Experimental Section), all metal ions showed fast complexation reactions. Taking into account the high number (10) of amine groups and the presence of many chelating units in L, speciation of complex systems was performed over a large range of metal/ligand molar ratios (see the Experimental Section) to accurately define the maximum number of each metal ion that can be bound by L as well as the lower-nuclearity complex species. The results showed that, among the metal ions here considered, only Cu^{2+} is able to form trinuclear complexes; all metal ions form mono- and binuclear species, with the exception of Pb^{2+}, for which only mononuclear ones were found. Ni^{2+}, Zn^{2+}, and Cd^{2+} give also rise to 3:2 metal/ligand complexes (Table 4). Distribution diagrams illustrating the relative percentages of complex species formed over the pH range of 2−12 are reported in Figures S3−S7 of the Supporting Information.

As can be seen from Table 4, the mononuclear systems are similar for all five metal ions, being constituted by the presence of ML^{2+} complexes in alkaline solution and by the formation of numerous protonated species at lower pHs. Lead also forms the $PbLOH^+$ hydroxo complex. The stability of the ML^{2+} complexes is consistent with the behavior of other polyamines, both linear and branched,[51] and varies in the order of Cu^{2+} > Ni^{2+} > Cd^{2+} > Zn^{2+} > Pb^{2+}. A quite similar stability trend was reported, for instance, for the linear hexamine 1,16-dimethyl-1,4,7,10,13,16-hexaazahexadecane (Me_2pentaen).[52] Despite that Me_2pentaen forms slightly more stable Ni^{2+} and Cu^{2+} complexes than L, the two ligands show a strict parallelism in complex stability (Figure S8 in the Supporting Information). In the case of Me_2pentaen, the ligand was shown to involve all of

dx.doi.org/10.1021/ic3025292 | Inorg. Chem. 2013, 52, 2125−2137

Table 4. Stability Constants of Metal Complexes with L in 0.10 M Me_4NCl at 298.1 ± 0.1 K

	Ni^{2+}	Cu^{2+}	Zn^{2+}	Cd^{2+}	Pb^{2+}
			log *K*		
$M^{2+} + L = ML^{2+}$	16.63(7)[a]	20.51(4)	14.17(6)	15.41(7)	9.43(5)
$ML^{2+} + H^+ = MHL^{3+}$	9.91(7)	9.85(5)	9.92(6)	9.64(7)	9.77(5)
$MHL^{3+} + H^+ = MH_2L^{4+}$	8.96(7)	8.81(5)	8.88(6)	8.84(8)	8.87(5)
$MH_2L^{4+} + H^+ = MH_3L^{5+}$	8.57(6)	8.18(5)	8.22(4)	7.87(8)	8.76(6)
$MH_3L^{5+} + H^+ = MH_4L^{6+}$	5.36(5)	6.15(2)	6.53(4)	5.68(2)	7.98(4)
$MH_4L^{6+} + H^+ = MH_5L^{7+}$	4.00(5)	3.68(3)	5.32(4)		6.58(8)
$ML^{2+} + OH^- = MLOH^+$					2.78(6)
$M^{2+} + HL^+ = MHL^{3+}$	16.38(7)	20.20(5)	13.93(6)	14.89(7)	9.04(5)
$M^{2+} + H_2L^{2+} = MH_2L^{4+}$	15.37(7)	19.04(5)	12.84(6)	13.76(8)	7.94(5)
$M^{2+} + H_3L^{3+} = MH_3L^{5+}$	14.68(6)	17.96(5)	11.80(4)	12.37(3)	7.44(6)
$M^{2+} + H_4L^{4+} = MH_4L^{6+}$	10.82(5)	14.89(2)	9.11(4)	8.83(2)	6.20(4)
$M^{2+} + H_5L^{5+} = MH_5L^{7+}$	6.25(5)	10.00(3)	5.86(4)		4.21(8)
$2M^{2+} + L = M_2L^{4+}$	24.35(7)	34.87(5)	22.06(5)	21.28(5)	
$ML^{2+} + M^{2+} = M_2L^{4+}$	7.72(7)	14.36(9)	7.89(6)	5.87(5)	
$M_2L^{4+} + H^+ = M_2HL^{5+}$	8.81(7)	8.21(5)	8.59(5)	8.99(5)	
$M_2HL^{5+} + H^+ = M_2H_2L^{6+}$	5.23(8)	5.45(3)	6.78(8)		
$M_2L^{4+} + OH^- = M_2LOH^{3+}$	2.77(8)	5.17(5)	4.50(6)	2.85(8)	
$M_2LOH^{3+} + OH^- = M_2L(OH)_2^{2+}$		2.86(5)			
$3M^{2+} + 2L = M_3L_2^{6+}$	48.92(9)		40.4(1)	40.6(1)	
$M_3L_2^{6+} + H^+ = M_3HL_2^{7+}$	8.78(9)		9.4(1)	9.7(1)	
$M_3HL_2^{7+} + H^+ = M_3H_2L_2^{8+}$	8.67(9)		8.2(1)	8.5(1)	
$M_2L^{4+} + ML^{2+} = M_3L_2^{6+}$	7.9(1)		4.2(1)	3.9(1)	
$2ML^{2+} + M^{2+} = M_3L_2^{6+}$	15.7(1)		12.1(1)	9.8(1)	
$3M^{2+} + L = M_3L^{6+}$		42.74(3)			
$M_3L^{6+} + OH^- = M_3LOH^{5+}$		6.1(1)			
$M_2L^{4+} + M^{2+} = M_3L^{6+}$		7.87(8)			

[a]Values in parentheses are the standard deviations on the last significant figures.

its six donor atoms in the coordination to Ni^{2+} and Cd^{2+}, while five of them are included in the coordination sphere of Cu^{2+} and Zn^{2+}, and only four are used to bind Pb^{2+}. The same trend of stability and the same coordination numbers were also shown by complexes of the branched hexamine penten $(H_2NCH_2CH_2)_2NCH_2CH_2N(CH_2CH_2NH_2)_2$ with all of these metal ions, but ZnL^{2+},[53] which exhibits the same stability and the same ligand hexacoordination of CdL^{2+} (Figure S8, Supporting Information).[53a,c] Accordingly, the number of donor atoms involved by L in the coordination to the present metal ions would be six for NiL^{2+} and CdL^{2+}, five for CuL^{2+} and ZnL^{2+}, and four for PbL^{2+}. A support to this behavior can be furnished by the equilibrium constants for the complex protonation processes. As can be seen from Table 4, the first three protonation constants of NiL^{2+} and CdL^{2+} are very high and fall in the range of basicity shown by the primary amine groups of the metal-free ligand, the first tertiary amine group of the free ligand being protonated having a protonation constant of log *K* = 5.69 (Table 1). The fourth protonation constants of these complexes (Table 4) are much smaller than the previous ones, and their values are consistent with protonation occurring on tertiary not-coordinated nitrogen atoms (Table 1). NiL^{2+} undergoes a further protonation stage associated with a small equilibrium constant that can be ascribed to protonation of a coordinated nitrogen atom. That is, in NiL^{2+}, there are three primary and one tertiary nitrogen atom not involved in the coordination while the remaining six ligand donor atoms should be comprised in the coordination sphere of the metal ion. Cd^{2+} does not bear a fifth protonation, but its behavior in the first four stages is identical to that of NiL^{2+}.

The interaction of Ni^{2+} with L can also be followed by monitoring the spectral changes of the metal ion occurring in the UV−vis region upon complexation at different pH values. Figure 8 displays the electronic spectra of the Ni^{2+}/L system in

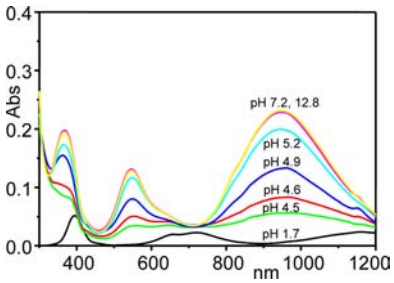

Figure 8. Adsorption spectra of the Ni^{2+}/L system at various pH values. $[Ni^{2+}]$ = 0.010 M, [L] = 2$[Ni^{2+}]$, 298 K.

the 1.7−12.8 pH range. The spectrum of the mauve NiL^{2+} complex, obtained at pH 12.8 in the presence of a 2-fold excess of ligand ([L] = 2$[Ni^{2+}]$) to depress the formation of complexes with a metal/ligand stoichiometry different from 1:1, is the typical spectrum of a Ni^{2+} octahedral, high-spin complex, being constituted by three bands at 947 nm (ε = 22.9 M^{-1} cm^{-1}), 546 nm (ε = 12.8 M^{-1} cm^{-1}), and 367 nm (ε = 19.3 M^{-1} cm^{-1}). The position of these bands does not change on progressively lowering the solution pH down to 4.5, while the mono- to tetraprotonated forms of NiL^{2+} are successively formed, confirming that the first four complex protonation events do not modify the coordination environment of the metal ion. Unfortunately, it is not possible to identify the

dx.doi.org/10.1021/ic3025292 | *Inorg. Chem.* 2013, 52, 2125−2137

spectral modifications due to the formation of the pentaprotonated NiH_5L^{7+} complex, since this species is formed in very small amounts even under the experimental conditions ([L] = 2[Ni^{2+}]) adopted to record the spectra.

In the case of CuL^{2+}, the analysis of complex protonation constants suggests that the first four protonation stages occur on primary not-coordinated nitrogen atoms, but the fifth one is too small to be assigned to a nitrogen atom not involved in metal coordination. Nevertheless, the analysis of the electronic spectra of the Cu^{2+} complexes is consistent with all protonation stages occurring on uncoordinated nitrogen atoms. The electronic spectrum of CuL^{2+} (Figure 9), recorded at pH

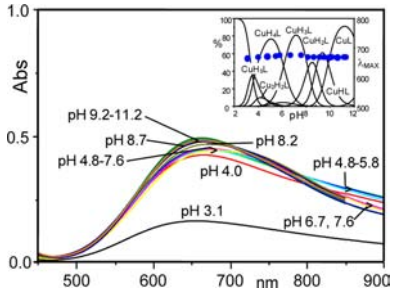

Figure 9. Adsorption spectra of the Cu^{2+}/L system at various pH values. [Cu^{2+}] = 0.0026 M, [L] = 2[Cu^{2+}], 298 K. Inset: values of λ_{max} at different pHs superimposed to the distribution diagram of the complex species formed in the system.

11.2 with a solution containing a 2-fold excess of ligand to reduce the formation of complexes with a metal/ligand stoichiometry different from 1:1, is characterized by a single broad band centered at 666 nm (ε = 181 M^{-1} cm^{-1}), whose position shows a very small variation on lowering the solution pH (inset Figure 9), that is, when protonated complexes are formed. It is well-known that the position of the band in the electronic spectra of Cu^{2+} complexes is very sensible to the number of coordinated amine groups.[54,55] Accordingly, the invariance of the pick position observed for CuL^{2+} and all of its protonated forms, from $CuHL^{3+}$ to CuH_5L^{7+}, can be taken as evidence of the pentacoordination of L in all of these complexes. In particular, this band at (or close to) 666 nm falls in the range (580−670 nm) usually observed for pentacoordinated polyamine complexes with Cu^{2+} in square-pyramidal (*sp*) geometry.[54−56] Nevertheless, the spectra recorded at pH ≤ 5.8 exhibit an increase of absorbance in the lower-energy region (Figure 9), which can be reasonably ascribed to the presence of minor forms with a trigonal-bipyramidal (*tbp*) geometry according to the general behavior of *tbp* polyamine complexes of Cu^{2+} that show the absorption band at 780−950 nm.[54,55,57] Such *tbp* component(s) could be some $Cu_2H_2L^{6+}$ complex, whose formation in small amounts occurs in that pH region despite the excess of ligand used to record the spectra, and/or some minor *tbp* form(s) of mononuclear complexes in the highest protonation state (CuH_4L^{6+}, CuH_5L^{7+}) that is(are) in equilibrium with major *sp* forms. As we will see further on, the first possibility seems to be more likely, since the polynuclear Cu^{2+} complexes of L in solution show a *tbp* component.

As for ZnL^{2+}, the analysis of complex protonation constants supports the previously deduced number (5) of ligand donor atoms involved in the coordination to this metal ion. Nevertheless, the fifth protonation constant (log *K* = 5.32) is significantly higher than that found for the analogous protonation stage involving the Cu^{2+} complex (log *K* = 3.68) for which the pentacoordination of the ligand has been demonstrated in all protonated forms. Unfortunately, for the Zn^{2+} complex, a direct information on the modifications that can occur in the coordination sphere of the metal ion upon complex protonation is not available, since the UV−vis spectrum of the complex is completely silent and ^{1}H NMR spectra recorded at different pH values are not amenable to analysis due to the broadening and overlapping of ligand signals observed upon complexation. For this reason, we undertook a modeling study on the ZnH_5L^{7+} complex by means of QM/MM calculations in which the water solvent molecules were treated in an explicit manner. The minimum energy structure calculated for this complex (Figure 10) shows that only four

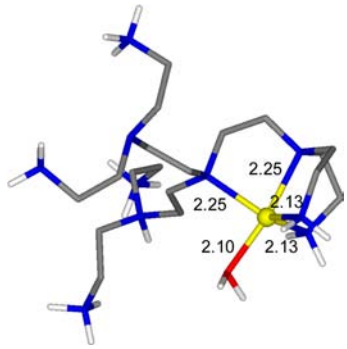

Figure 10. Minimum energy structures calculated for the ZnH_5L^{7+} complex.

nitrogen atoms of the ligand, including the central tertiary nitrogen and three nitrogens of a connected triamine unit, participate in the coordination to Zn^{2+}, which completes its pentacoordinated environment with a water molecule.

Reasonably, the repulsion generated by the five ammonium groups of this complex causes the cleavage of one coordinative bond, allowing the metal ion to move far from the ammonium groups, thus producing a stabilization of the protonated species. The overall organization of the complex defines a nest, surrounded by the positive charges of the metal ion and three ammonium groups, which offers open access to solvent molecules (Figure S9, Supporting Information) and suggests the possibility of hosting anionic species.

In the case of PbL^{2+}, for which, as commented above, a tetracoordination of the ligand can be inferred on the basis of its stability, the observed five protonated species appear to be formed upon stepwise protonation of five uncoordinated primary amine groups, the corresponding protonation constants (log *K* = 9.77−6.58, Table 4) being considerably higher than the limiting value (log *K* = 5.69, Table 1) found for protonation of the first tertiary nitrogen of the metal-free ligand. Hence, in PbH_5L^{7+}, 4 out of the 10 ligand nitrogen atoms should be coordinated to the metal ion, 5 (primary ones) are protonated, and 1 is neither coordinated nor protonated. The formation of the hydroxylated $PbLOH^+$ complex is consistent with the low number of donor atoms used by L to bind Pb^{2+}.

As already noted, all of these metal ions, but Pb^{2+}, form binuclear complexes. The complexation models for the formation of binuclear species are similar, being composed of M_2L^{4+}, M_2HL^{5+}, $M_2H_2L^{6+}$, and M_2LOH^{3+} (M = Ni, Cu, Zn, Cd) species. Only Cd^{2+} does not form $M_2H_2L^{6+}$, whereas Cu^{2+}

dx.doi.org/10.1021/ic3025292 | *Inorg. Chem.* 2013, 52, 2125−2137

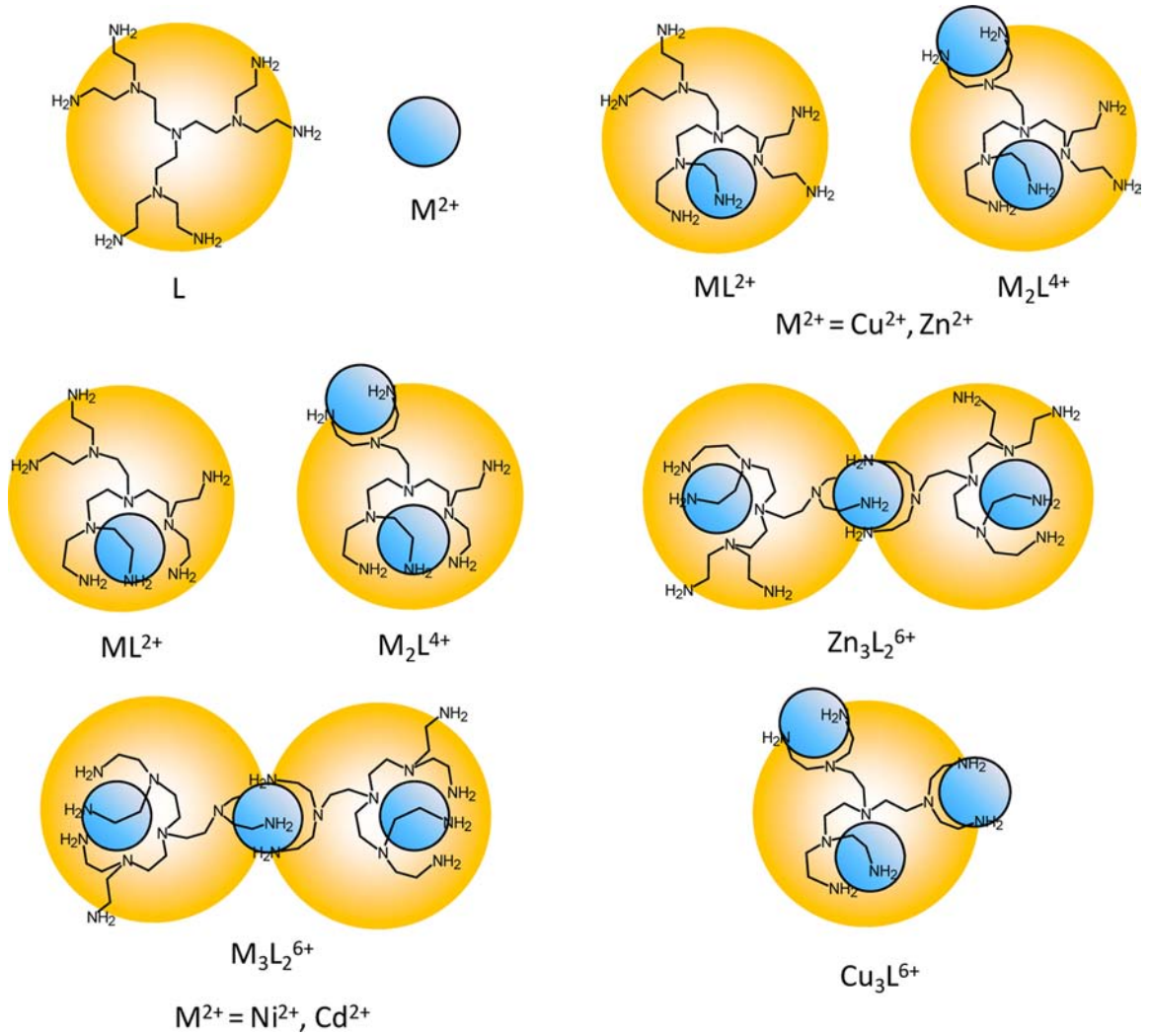

Figure 11. Schematic representation of the coordination environments suggested for the complexes formed by L in solution.

gives also rise to the dihydroxylated $Cu_2L(OH)_2^{2+}$ complex. The equilibrium constants for the binding of the second metal ion, according to the equilibrium $ML^{2+} + M^{2+} = M_2L^{4+}$, are intermediate between the values reported for the formation of 1:1 complexes of the same metal ions, respectively, with di- and triamine ligands, such as ethylenediamine and diethylenetriamine,[51] containing ethylenic spacers between amino groups like in L. A similar behavior could be explained by considering that the second metal ion binds to a triamine branch of the ligand without producing significant modifications in the coordination environment of the first, already coordinated, metal ion. As a matter of fact, according to the above considerations, all ML^{2+} (M = Ni, Cu, Zn, Cd) should contain a free (not coordinated) triamine branch. Furthermore, considering that some electrostatic repulsion is exerted between the two metal ions in the binuclear M_2L^{4+} complex, the equilibrium constant for the binding of a metal ion to the uncoordinated triamine branch of ML^{2+} is expected to be smaller than the constant for the binding of the same metal ion to free diethylenetriamine, while, if the second metal ion would be coordinated to only two contiguous nitrogen atoms of ML^{2+}, the corresponding equilibrium constant could not be greater than that reported for the binding of M^{2+} by ethylenediamine. On the basis of such considerations, one nitrogen atom of L should not be coordinated in Ni_2L^{4+} and Cd_2L^{4+}, whereas two of them should be free in Cu_2L^{4+} and Zn_2L^{4+}. Accordingly, all of these complexes give rise to first protonation stages featuring equilibrium constants typical of primary amine groups. This is the only protonation event sustained by Cd_2L^{4+}, while Ni_2L^{4+} is involved in a second protonation step characterized by a lower equilibrium constant, which is consistent with protonation of a coordinated amine group. Also, Cu_2L^{4+} and Zn_2L^{4+} are involved in a second protonation step, which, at least in the case of Zn_2L^{4+}, can be ascribed to protonation of another not-coordinated primary amine group (Table 4). Schematic structures suggested for mono- and binuclear complexes are shown in Figure 11. Such coordination schemes are consistent with the coordination features observed in the crystal structures previously described.

A salient characteristic of this ligand is its ability to form complexes with a 3:2 metal-to-ligand stoichiometry ($M_3L_2^{6+}$, $M_3HL_2^{7+}$, $M_3H_2L_2^{8+}$) in the presence of Ni^{2+}, Zn^{2+}, and Cd^{2+}. The propensity to form such complexes with Ni^{2+} is so high that the $Ni_3L_2^{6+}$ complex, whose crystal structure is described above, is the unique species present in solution above pH 10 (Figure S3b, Supporting Information) for a Ni^{2+}/L molar ratio equal to 1.5. This species competes very strongly with the formation of Ni_2L^{4+} and Ni_2LOH^{3+}, making rather complicated the identification of such species and the determination of their stability constants (see the Experimental Section). Although of

dx.doi.org/10.1021/ic3025292 | Inorg. Chem. 2013, 52, 2125−2137

lower stability (Table 4), also the 3:2 complexes with Zn^{2+} and Cd^{2+} are important species in solution when such stoichiometry is accomplished (Figures S5 and S6, Supporting Information). All $M_3L_2^{6+}$ (M = Ni, Zn, Cd) complexes participate in two protonation stages, and the relevant protonation constants, varying in the range of log K = 8.2−9.4 (Table 4), testify that two primary amine groups in each $M_3L_2^{6+}$ complex are not involved in metal coordination, in agreement with the structure observed in the solid state for $Ni_3L_2^{6+}$ (Figure 3). The whole set of information suggests that this structure is maintained in solution, being also representative of the structures assumed by $Zn_3L_2^{6+}$ and $Cd_3L_2^{6+}$. These complexes can be though as resulting from coordinative interaction between M_2L^{4+} and ML^{2+}, or from bridging coordination of M^{2+} between two ML^{2+} units (Figure 11). The equilibrium constants for such reactions (Table 4) confirms the great propensity of Ni^{2+} to form the $Ni_3L_2^{6+}$ complex. Solutions of $Ni_3L_2^{6+}$ show a typical spectrum of a Ni^{2+} octahedral, high-spin complex, being constituted by three bands at 944 nm (42.1 M^{-1} cm^{-1}), 544 nm (29.3 M^{-1} cm^{-1}), and 359 (51.6 M^{-1} cm^{-1}) (Figure S10, Supporting Information). In such $M_3L_2^{6+}$ complexes, the central metal ion is octahedrally coordinated to two triamine branches pertaining to different ligand molecules. Accordingly, among the metal ions here studied and capable of producing polynuclear species, only Cu^{2+} is not able to assemble similar 3:2 complexes with L, in agreement with the low tendency of Cu^{2+} to bind two tridentate ligand molecules in consequence of the Jahn−Teller distortion typical of d^9 metal ions.

Last, but not least, the formation of trinuclear Cu^{2+} complexes enriches the picture of complexation properties shown by this G-2 poly(ethylene imine) dendrimer. The equilibrium constant (log K = 7.87, Table 4) for the coordination of the third Cu^{2+} ion (Cu_2L^{4+} + Cu^{2+} = Cu_3L^{6+}) is large enough to make Cu_3L^{6+} the prominent, almost unique species around pH 6 in solutions containing L and Cu^{2+} in a 1:3 molar ratio, the trinuclear complex giving rise to Cu_3LOH^{5+} at higher pHs (Figure S3c, Supporting Information). According to the structure suggested for Cu_2L^{4+} (Figure 11), only two ligand donor atoms are not coordinated in this complex. The equilibrium constant for the binding of the third Cu^{2+} ion (log K = 7.87, Table 4) is then mostly determined by the favorable coordinative contribution from these two nitrogen atoms reduced by the energetic cost for rearrangement of the complex structure and increased electrostatic repulsion between metal ions. As a matter of fact, this equilibrium constant is lower, by about 2 orders of magnitude, than the constants for the binding of Cu^{2+} by diamine ligands, such as ethylenediamine and its N-alkylated derivatives.[S1] To be noted is also the absence of protonated forms of the trinuclear complex, which can be reasonably interpreted as evidence that all 10 nitrogen atoms of the ligand participate in the coordination to the three metal ions.

The crystal structure of the $[Cu_3LCl(OH)_{0.5}(NO_3)_{0.5}ox]^{2+}$ complex described above (Figure 5) shows that each Cu^{2+} cation is coordinated to a single triamine branch of the ligand, one of them also including the innermost tertiary nitrogen atom in its coordination sphere. A similar arrangement of metal ions, deprived of coordinated anions, seems to be a good model for the structure of Cu_3L^{6+} in solution (Figure 11). It involves all ligand donors, achieving the most equitable distribution among the metal ions, and allows the three metal centers to stay apart from each other to minimize the electrostatic repulsion between them. Reasonably, this crystal structure can also be taken as a model for the trinuclear hydroxo Cu_3LOH^{5+} complex, once all coordinated anions, but OH^-, are removed.

The electronic spectrum of Cu_3L^{6+} (Figure S11 in the Supporting Information) is characterized by a maximum at 663 nm (ε = 304 M^{-1} cm^{-1}) with a pronounced shoulder at lower energy (~870 nm) denoting the presence of Cu^{2+} ions in both *sp* and *tbp* coordination geometries within the solvated complex.

When the metal ion binding properties of this poly(ethylene imine) ligand and its analogous linear[S2] and macrocyclic[S2d,S8] molecules able to form polynuclear complexes are compared, we find that the dendrimeric structure endows L with a greater nucleating ability and a greater ability to form highly protonated metal complexes, although the complex stability is commonly lower than that of these linear and macrocyclic polyamines.

CONCLUSIONS

To sum up, we have shown that the G-2 poly(ethylene imine) dendrimer L, based on ammonia as the initiating core molecule, exhibits special properties in the formation of metal ion complexes. Mono-, bi-, and trinuclear complexes, as well as 3:2 metal/ligand species, are formed, depending on the nature of the metal cation and the metal/ligand molar ratio. Metal ion binding can take place either in the inner region or on the surface of the dendrimer molecules. Coordinated metal cations decorating the dendrimer surface can direct the self-assembly of dendrimer units into monodimensional aggregates according to two different ion-directed association routes developing under thermodynamic control: (a) aggregation via metal ions shared by the surfaces of contiguous dendrimer molecules and (b) aggregation via chelating ligands bridging surface metal ions pertaining to contiguous dendrimer molecules. The first association mode was displayed by the crystal structure of the linear $Ni_3L_2^{6+}$ assembly. Interestingly, $Ni_3L_2^{6+}$ and the analogous nanostructures formed by Zn^{2+} and Cd^{2+} are stable in aqueous solution. The second mode was achieved by the action of oxalate anions (ox) on the trinuclear Cu_3L^{6+} complex, as displayed by the crystal structure of $[Cu_3LCl(OH)_{0.5}(NO_3)_{0.5}ox]Cl_{1.5}(NO_3)_{0.5}\cdot 5.5H_2O$ showing zigzag ···Cu_3L^{6+}-ox-Cu_3L^{6+}-ox··· hierarchically nanostructured chains that self-organize into two-dimensional sheets. In the two cases, both mono- and two-dimensional aggregation is triggered by the action of ionic species behaving either as functional groups on the dendrimer surface (metal ions) or as the glue (metal ions, oxalate) that sticks together dendrimer units.

These two routes, which are shown here to be effective with a G-2 dendrimer, are expected to function also with higher-generation analogues; in particular, this applies to the second route, which does not require a special flexibility of the dendrimer molecule. Accordingly, they provide coordinative methods for the creation of novel families of nanostructured functional materials that could prove useful for the development of the material science-based approach to nanotechnology.

ASSOCIATED CONTENT

Supporting Information

pH dependence of the ^1H NMR signals of L, distribution diagrams of the complex species formed in the systems M^{2+}/L (M = Ni, Cu, Zn, Cd, Pb), adsorption spectra of $Ni_3L_2^{6+}$ and Cu_3L^{6+}, X-ray crystallographic data including CIF files, and ORTEP drawings displaying the thermal ellipsoids of $Ni_3L_2^{6+}$

dx.doi.org/10.1021/ic3025292 | Inorg. Chem. 2013, 52, 2125−2137

and $[Cu_3LCl(OH)_{0.5}(NO_3)_{0.5}ox]^{2+}$. This material is available free of charge via the Internet at http://pubs.acs.org.

AUTHOR INFORMATION

Corresponding Author

*E-mail: antonio.bianchi@unifi.it.

Notes

The authors declare no competing financial interest.

REFERENCES

(1) Tomalia, D. A. *J. Nanopart. Res.* **2009**, *11*, 1251−1310.

(2) Books: (a) Vögtle, F.; Richardt, G.; Werner, N. *Dendrimer Chemistry*; Wiley-VCH: Weinheim, 2007. (b) Boas, U.; Christensen, J. B.; Heegaard, P. M. H. *Dendrimers in Medicine and Biotechnology: New Molecular Tools*; RSC Publishing: Cambridge, U.K., 2006. (c) Gade, L. H., Ed. *Dendrimer Catalysis*; Topics in Organometallic Chemistry; Springer: Berlin, 2006; Vol. *20*. (d) Newkome, G. R.; Moorefield, C. N.; Vögtle, F. *Dendritic Molecules: Concepts, Syntheses, Perspectives*; VCH: Weinheim, 1996. (e) Schalley, C. A., Vögtle, F., Eds. *Dendrimers V: Functional and Hyperbranched Building Blocks, Photophysical Properties, Applications in Materials and Life Sciences*; Topics in Current Chemistry; Springer: Berlin, 2003; Vol. *228*. (f) Vögtle, F., Schalley, C. A., Eds. *Dendrimers IV: Metal Coordination, Self Assembly, Catalysis*; Topics in Current Chemistry; Springer: Berlin, 2001; Vol. *217*. (g) Vögtle, F., Ed. *Dendrimers III: Design, Dimension, Function*; Topics in Current Chemistry; Springer: Berlin, 2001; Vol. *212*. (h) Vögtle, F., Ed. *Dendrimers II: Architecture, Nanostructure and Supramolecular Chemistry*; Topics in Current Chemistry; Springer: Berlin, 2000; Vol. *210*. (i) Vögtle, F., Ed. *Dendrimers*; Topics in Current Chemistry; Springer: Berlin, 1998; Vol. *210*.

(3) Reviews: (a) Tomalia, D. A.; Naylor, A. M.; Goddard, W. A., III *Angew. Chem., Int. Ed.* **1990**, *29*, 138−175. (b) Bergamini, G.; Marchi, E.; Ceroni, P. *Coord. Chem. Rev.* **2011**, *255*, 2458−2468. (c) Konkolewicz, D.; Monteiro, M. J.; Perrier, S. *Macromolecules* **2011**, *44*, 7067−7087. (d) Tomalia, D. A. *Adv. Mater.* **1994**, *6*, 529−539. (e) Fréchet, J. M. *Science* **1994**, *263*, 1710−1715. (f) Zeng, F.; Zimmerman, S. C. *Chem. Rev.* **1997**, *97*, 1681−1712. (g) Tomalia, D. A. *J. Nanopart. Res.* **2009**, *11*, 1251−1310. (h) Caminade, A.-M.; Majoral, J.-P. *Chem. Soc. Rev.* **2010**, *39*, 2034−2047. (i) Rolland, O.; Turrin, C.-O.; Caminade, A.-M.; Majoral, J.-P. *New J. Chem.* **2009**, *33*, 1809−1824. (j) Astruc, D.; Ornelas, C.; Ruiz, J. *Chem.—Eur. J.* **2009**, *15*, 8936−8944. (k) Astruc, D.; Boisselier, E.; Ornelas, C. *Chem. Rev.* **2010**, *110*, 1857−959. (l) Astruc, D.; Lu, F.; Ruiz Aranzaes, J. *Angew. Chem., Int. Ed.* **2005**, *44*, 7852−7872. (m) Stiriba, S.-E.; Frey, H.; Haag, R. *Angew. Chem., Int. Ed.* **2002**, *41*, 1329−1334. (n) Frey, H.; Lach, C.; Lorenz, K. *Adv. Mater.* **1998**, *10*, 279−293. (o) Bronstein, L. M.; Shifrina, Z. B. *Chem. Rev.* **2011**, *111*, 5301−5344. (p) Mekelburger, H. B.; Jaworek, W.; Vögtle, F. *Angew. Chem., Int. Ed. Engl.* **1992**, *31*, 1571−1576. (q) Balzani, V.; Bergamini, G.; Ceroni, P.; Vögtle, F. *Coord. Chem. Rev.* **2007**, *251*, 525−535.

(4) (a) Guillot-Nieckowski, M.; Eisler, S.; Diederich, F. *New J. Chem.* **2007**, *31*, 1111−1127. (b) Feber, D. *Science* **2001**, *294*, 1638−1642. (c) Kukowska-Latallo, J. F.; Bielinska, A. U.; Johnson, J.; Spindler, R.; Tomalia, D. A.; Baker, J. R. *Proc. Natl. Acad. Sci. U.S.A.* **1996**, *93*, 4897−4902.

(5) Amir, R. J.; Albertazzi, L.; Willis, J.; Khan, A.; Tang, T.; Howker, C. J. *Angew. Chem., Int. Ed.* **2011**, *50*, 3425−3429.

(6) (a) Rupp, R.; Rosenthal, S. L.; Stanberry, L. R. *Int. J. Nanomed.* **2007**, *2*, 561−566. (b) Roy, R. *Curr. Opin. Struct. Biol.* **1996**, *6*, 692−702.

(7) Albertazzi, L.; Storti, B.; Marchetti, L.; Beltram, F. *J. Am. Chem. Soc.* **2010**, *132*, 18158−18167.

(8) (a) Tong, G. J.; Hsiao, S. C.; Carrico, Z. M.; Francis, M. B. *J. Am. Chem. Soc.* **2009**, *131*, 11174−11178. (b) Wesley, W.; Hsiao, S. C.; Carrico, Z. M.; Francis, M. B. *Angew. Chem., Int. Ed.* **2009**, *48*, 9493−9497. (c) Mann, S. *Nat. Mater.* **2009**, *8*, 781−792. (d) Okuro, K.; Kinbara, K.; Tsumoto, K.; Ishii, N.; Aida, T. *J. Am. Chem. Soc.* **2009**, *131*, 1626−1627. (e) Herrero, M. A.; Toma, F. M.; Al-Jamal, K. T.; Kostarelos, K.; Bianco, A.; Da Ros, T.; Bano, F.; Casalis, L.; Scoles, G.; Prato, M. *J. Am. Chem. Soc.* **2009**, *131*, 9843−9848. (f) Yoo, P. J.; Nam, K. T.; Qi, J.; Lee, S.-K.; Park, J.; Belcher, A. M.; Hammond, P. T. *Nat. Mater.* **2006**, *5*, 234−240. (g) Ercolani, G. *J. Am. Chem. Soc.* **2003**, *125*, 16097−16103. (h) Whitesides, G. M.; Grzybowski, B. *Science* **2002**, *295*, 2418−2421.

(9) Ottaviani, M. F.; Bossmann, S.; Turro, N. J.; Tomalia, D. A. *J. Am. Chem. Soc.* **1994**, *116*, 661−671.

(10) Jarvis, N. V.; Wagener, J. M. *Talanta* **1995**, *42*, 219−226.

(11) Ottaviani, M. F.; Montalti, F.; Turro, N. J.; Tomalia, D. A. *J. Phys. Chem. B* **1997**, *101*, 158−166.

(12) Bosman, A. W.; Schenning, A. P. H. J.; Jansenn, R. A. J.; Meijer, E. W. *Chem. Ber./Recl.* **1997**, *130*, 725−728.

(13) Zhao, M.; Sun, L.; Crooks, R. M. *J. Am. Chem. Soc.* **1998**, *120*, 4877−4878.

(14) Diallo, M. S.; Balogh, L.; Shafagati, A.; Johnson, J. H.; Goddard, W. A., III; Tomalia, D. A. *Environ. Sci. Technol.* **1999**, *33*, 820−824.

(15) Vassilev, K.; Ford, W. T. *J. Polym. Sci., Part A* **1999**, *37*, 2727−2736.

(16) Balogh, L.; Valluzzi, R.; Laverdure, K. S.; Gido, S. P.; Hagnauer, G. L.; Tomalia, D. A. *J. Nanopart. Res.* **1999**, *1*, 353−368.

(17) Zhao, M.; Crooks, R. M. *Chem. Mater.* **1999**, *33*, 820−824.

(18) Floriano, P. N.; Noble, C. O., IV; Schoonmaker, J. M.; Poliakoff, E. D.; McCarley, R. L. *J. Am. Chem. Soc.* **2001**, *123*, 10545−10553.

(19) Crooks, R. M.; Zhao, M.; Sun, L.; Chechik, V.; Yeung, L. K. *Acc. Chem. Res.* **2001**, *34*, 181−190.

(20) Ottaviani, M. F.; Valluzzi, R.; Balogh, L. *Macromolecules* **2002**, *35*, 5105−5115.

(21) Krämer, M.; Pérignon, N.; Haag, R.; Marty, J.-D.; Thomann, R.; Lauth-de Viguere, N.; Mingotaud, C. *Macromolecules* **2005**, *38*, 8308−8315.

(22) Vassilev, K.; Turmanova, S.; Dimitrova, M.; Boneva, S. *Eur. Polym. J.* **2009**, *45*, 2269−2278.

(23) Mitran, E.; Dellinger, B.; McCarley, R. L. *Chem. Mater.* **2010**, *22*, 6555−6563.

(24) Wan, H.; Li, S.; Konovalova, T. A.; Zhou, Y.; Thrasher, J. S.; Dixon, D. A.; Street, S. C. *J. Phys. Chem. C* **2009**, *113*, 5358−5367.

(25) Branchi, B.; Ceroni, P.; Balzani, V.; Bergamini, G.; Klaerner, F.-K.; Voegtle, F. *Chem.—Eur. J.* **2009**, *15*, 7876−7882.

(26) Mankbadi, M. R.; Barakat, M. A.; Ramadan, M. H.; Woodcock, H. L.; Kuhn, J. N. *J. Phys. Chem. B* **2011**, *115*, 13534−13540.

(27) Pande, S.; Crooks, R. M. *Langmuir* **2011**, *27*, 9609−9613.

(28) (a) Peñas-Sanjuan, A.; López-Garzón, R.; López-Garzón, J.; Pérez-Mendoza, M.; Melguizo, M. *Carbon* **2012**, *50*, 2350−2352. (b) Peñas-Sanjuan, A. Surface functionalization of activated carbon by non-conventional techniques and its potential applications as pollutant and catalytic metal scavenger, Ph.D. Thesis, University of Jaén, Jaén, Spain, 2011.

(29) Garzoni, M.; Cheval, N.; Fahmi, A.; Danani, A.; Pavan, G. M. *J. Am. Chem. Soc.* **2012**, *134*, 3349−3357.

(30) (a) Tomalia, D. A. *New J. Chem.* **2012**, *36*, 264−281. (b) Türp, D.; Nguyen, T.-T.-T.; Baumgarten, M.; Müllen, K. *New J. Chem.* **2012**, *36*, 282−298. (c) Ju, R.; Tessier, M.; Olliff, L.; Woods, R.; Summers, A.; Geng, Y. *Chem. Commun.* **2011**, *47*, 268−270. (d) Qi, X.; Xue, C.; Huang, X.; Huang, Y.; Zhou, X.; Li, H.; Liu, D.; Boey, F.; Yan, Q.; Huang, W.; De Feyter, S.; Müller, K.; Zhang, H. *Adv. Funct. Mater.* **2010**, *20*, 43−49. (e) Percec, V.; Wilson, D. A.; Leowanawat, P.; Wilson, C. J.; Hughes, A. D.; Kaucher, M. S.; Hammer, D. A.; Levine, D. H.; Kim, A. J.; Bates, F. S.; Davis, K. P.; Lodge, T. P.; Klein, M. L.; De Vane, R. H.; Aqad, E.; Rosen, B. M.; Argintau, A. O.; Sienkowska, M. J.; Rissanen, K.; Nummelin, S.; Ropponen, J. *Science* **2010**, *328*, 1009−1014. (f) Franc, G.; Badetti, E.; Colliere, V.; Majoral, J.-P.; Sebastian, R. M.; Caminade, A.-M. *Nanoscale* **2009**, *1*, 233−237. (g) Hermans, T. M.; Broeren, M. A. C.; Gomopoulos, N.; van der Schoot, P.; van Genderen, M. H. P.; Sommerdijk, N. A. J. M.; Fytas, G.; Meijer, E. W. *Nat. Nanotechnol.* **2009**, *4*, 721−726. (h) Wang, P.; Moorefield, C. N.; Jeong, K. U.; Hwang, S.-H.; Sinam, L.; Cheng, S. Z. D.; Newkome, G. R. *Adv. Mater.* **2008**, *20*, 1381−1385. (i) Fahmi, A.;

D'Aleo, A.; Williams, R. M.; De Cola, L.; Gindy, N.; Vögtle, F. *Langmuir* **2007**, *23*, 7831−7835.
(31) Tomalia, D. A.; Dewalt, J. R. U.S. Patent 4,631,339, 1986. Tomalia, D. A. European Patent 0115771, 1984.
(32) Martin, A. E.; Ford, T. M.; Bullkowski, J. E. *J. Org. Chem.* **1982**, *47*, 412−415.
(33) Fontanelli, M.; Micheloni, M. *Proceedings of the I Spanish-Italian Congress on Thermodynamics of Metal Complexes*; Diputación de Castellón: Castellón (Spain), 1990.
(34) Gran, G. *Analyst (London)* **1952**, *77*, 661−671.
(35) Gans, P.; Sabatini, A.; Vacca, A. *Talanta* **1996**, *43*, 1739−1753.
(36) Hall, J. P.; Izatt, R. M.; Christensen, J. J. *J. Phys. Chem.* **1963**, *67*, 2605−2608.
(37) Gans, P.; Sabatini, A.; Vacca, A. *J. Solution Chem.* **2008**, *37*, 467−476.
(38) Covington, A. K.; Paabo, M.; Robinson, R. A.; Bates, R. G. *Anal. Chem.* **1968**, *40*, 700−706.
(39) *ABSPACK*; Oxford Diffraction Ltd.: Oxford, U.K.
(40) Burla, M. C.; Caliandro, R.; Camalli, M.; Carrozzini, B.; Cascarano, G. L.; De Caro, L.; Giacovazzo, C.; Polidori, G.; Spagna, R. *J. Appl. Crystallogr.* **2005**, *38*, 381−388.
(41) Sheldrick, G. M.*SHELXL-97*; University of Göttingen; Göttingen, Germany, 1997.
(42) (a) Weiner, S. J.; Kollman, P. A.; Case, D. A.; Singh, U. C.; Ghio, C.; Alagona, G.; Profeta, S., Jr.; Weinerl, P. *J. Am. Chem. Soc.* **1984**, *106*, 765−784. (b) Weiner, S. J.; Kollman, P. A.; Nguyen, D. T.; Case, D. A. *J. Comput. Chem.* **1986**, *7*, 230−252.
(43) *Qsite*; Schrödinger, L. L. C.: New York. http://www.schrodinger.com.
(44) (a) Becke, A. D. *J. Chem. Phys.* **1993**, *98*, 1372−1380. (b) Becke, A. D. *J. Chem. Phys.* **1993**, *98*, 5684−5657. (c) Miehlich, B.; Savin, A.; Stoll, H.; Preuss, H. *Chem. Phys. Lett.* **1989**, *157*, 200−208.
(45) Hay, P. J.; Wadt, W. R. *J. Chem. Phys.* **1985**, *82*, 299−308.
(46) Banks, J. L.; Beard, H. S.; Cao, Y. X.; Cho, A. E.; Damm, W.; Farid, R.; Felts, A. K.; Halgren, T. A.; Mainz, D. T.; Maple, J. R.; Murphy, R.; Philipp, D. M.; Repasky, M. P.; Zhang, L. Y.; Berne, B. J.; Friesner, R. A.; Gallicchio, E.; Levy, R. M. *J. Comput. Chem.* **2005**, *26*, 1752−1780.
(47) Bencini, A.; Bianchi, A.; Garcia-España, E.; Micheloni, M.; Ramirez, J. A. *Coord. Chem. Rev.* **1999**, *188*, 97−156.
(48) Koper, G. J. M.; van Genderen, M. H. P.; Elissen-Román, C.; Baars, M. W. P. L.; Meijer, E. W.; Borkovec, M. *J. Am. Chem. Soc.* **1997**, *119*, 6512−6521.
(49) (a) *Cambridge Structural Database (CSD)*, version 5.32; Cambridge Crystallographic Data Centre: Cambridge, U.K. (accessed November 2011). (b) Allen, F. H. *Acta Crystallogr.* **2002**, *B58*, 380−388.
(50) Kadir, K.; Ahmed, T. M.; Noreús, D.; Eriksson, L. *Acta Crystallogr.* **2006**, *E62*, m1139−m1141.
(51) Smith, R. M.; Martell, A. E. *NIST Stability Constants Database*, Version 4.0; National Institute of Standards and Technology: Gaithersburg, MD, 1997.
(52) (a) Aragó, J.; Bencini, A.; Bianchi, A.; Garcia-España, E.; Micheloni, M.; Paoletti, P.; Ramirez, J. A.; Paoli, P. *Inorg. Chem.* **1991**, *30*, 1843−1849. (b) Aragó, J.; Bencini, A.; Bianchi, A.; Garcia-España, E.; Micheloni, M.; Paoletti, P.; Ramirez, J. A.; Rodriguez, A. *J. Chem. Soc., Dalton Trans.* **1991**, 3077−3083. (c) Bencini, A.; Bianchi, A.; Fusi, V.; Paoletti, P.; Valtancoli, B.; Andrés, A.; Aragó, J.; Garcia-España, E. *Inorg. Chim. Acta* **1993**, *204*, 221−225. (d) Andrés, A.; Bencini, A.; Carachalios, A.; Bianchi, A.; Dapporto, P.; Garcia-España, E.; Paoletti, P.; Paoli, P. *J. Chem. Soc., Dalton Trans.* **1993**, 3507−3513.
(53) (a) Paoletti, P.; Walser, R.; Vacca, A.; Schwarzenbach, G. *Helv. Chim. Acta* **1971**, *54*, 243−265. (b) Lubal1, P.; Musso, S.; Anderegg, G. *Helv. Chim. Acta* **2001**, *84*, 623−631. (c) Schwarzenbach, G.; Moser, P. *Helv. Chim. Acta* **1953**, *36*, 581−597.
(54) Lever, A. B. P. *Inorganic Electronic Spectroscopy*, 2nd ed.; Elsevier: New York, 1984.
(55) Ciampolini, M. *Struct. Bonding (Berlin)* **1969**, *6*, 52−93.
(56) (a) Algarra, G. A.; Basallote, M. G.; Castillo, C. E.; Clares, M. P.; Ferrer, A.; Garcia-España, E.; Llinares, J. M.; Soriano, C. *Inorg. Chem.* **2009**, *48*, 902−914. (b) Georgousis, Z. D.; Christidis, P. C.; Hadjipavlou-Litina, D.; Bolos, C. A. *J. Mol. Struct.* **2007**, *837*, 30−37. (c) Mautner, F. A.; Vicente, R.; Massoud, S. S. *Polyhedron* **2006**, *25*, 1673−1680. (d) Gérard, C.; Mohamadou, A.; Marrot, J.; Brandes, S.; Tabard, A. *Helv. Chim. Acta* **2005**, *88*, 2397−2412.
(57) (a) Thaler, F.; Hubbard, C. D.; Heinemann, F. W.; van Eldik, R.; Schindler, S.; Fabian, I.; Ditter-Klingemann, A. M.; Hahn, F. E.; Orving, C. *Inorg. Chem.* **1998**, *37*, 4042−4029. (b) Marzotto, A.; Ciccarese, A.; Clemente, D. A.; Valle, G. *J. Chem. Soc., Dalton Trans.* **1995**, 1461−1468. (c) Bencini, A.; Bianchi, A.; Borselli, A.; Chimici, S.; Ciampolini, M.; Dapporto, P.; Micheloni, M.; Nardi, N.; Paoli, P.; Valtancoli, B. *Inorg. Chem.* **1990**, *29*, 3282−3286. (d) Tyagi, S.; Hathaway, B. J. *J. Chem. Soc., Dalton Trans.* **1983**, 199−203.
(58) (a) Micheloni, M.; Paoletti, P.; Bianchi, A. *Inorg. Chem.* **1985**, *24*, 3702−3704. (b) Bianchi, A.; Mangani, S.; Micheloni, M.; Nanini, V.; Orioli, P.; Paoletti, P.; Seghi, B. *Inorg. Chem.* **1985**, *24*, 1182−1187. (c) Bencini, A.; Bianchi, A.; Garcia-España, E.; Giusti, M.; Micheloni, M.; Paoletti, P. *Inorg. Chem.* **1987**, *26*, 681−684. (d) Bencini, A.; Bianchi, A.; Garcia-España, E.; Giusti, M.; Mangani, S.; Micheloni, M.; Orioli, P.; Paoletti, P. *Inorg. Chem.* **1987**, *26*, 1243−1247. (e) Bencini, A.; Bianchi, A.; Garcia-España, E.; Mangani, S.; Micheloni, M.; Orioli, P.; Paoletti, P. *Inorg. Chem.* **1988**, *27*, 1104−1107. (f) Bencini, A.; Bianchi, A.; Castelló, M.; Di Vaira, M.; Faus, J.; Garcia-España, E.; Micheloni, M.; Paoletti, P. *Inorg. Chem.* **1989**, *28*, 347−351. (g) Bencini, A.; Bianchi, A.; Castelló, M.; Dapporto, P.; Faus, J.; Garcia-España, E.; Micheloni, M.; Paoletti, P.; Paoli, P. *Inorg. Chem.* **1989**, *28*, 3175−3181. (h) Bencimi, A.; Bianchi, A.; Micheloni, M.; Paoletti, P.; Garcia-España, E.; Niño, M. A. *J. Chem. Soc., Dalton Trans.* **1991**, 1171−1174.